Co-assembly nano pesticides of abamectin B1a and imidacloprid against *Ditylenchus destructor*

Rourou Wang,[a#] Fei Pan,[b#] Ming Niu,[a] Jing Zhou,[a] Haitao Long,[a] Lumei Pu,[a] Weibing Xu,[a*]

Runtian Ma,[a*] Haitao Yu[c]

[a] College of Science, Gansu Agricultural University, Lanzhou 730000, China;

[b] State Key Laboratory of Resource Insects, Institute of Apicultural Research, Chinese Academy of Agricultural Sciences, Beijing 100093, People's Republic of China.

[c] Institute of Plant Protection, Gansu Academy of Agricultural Sciences, Lanzhou,730070, China;

Correspondence: Weibing Xu, Email: xuwb@gsau.edu.cn

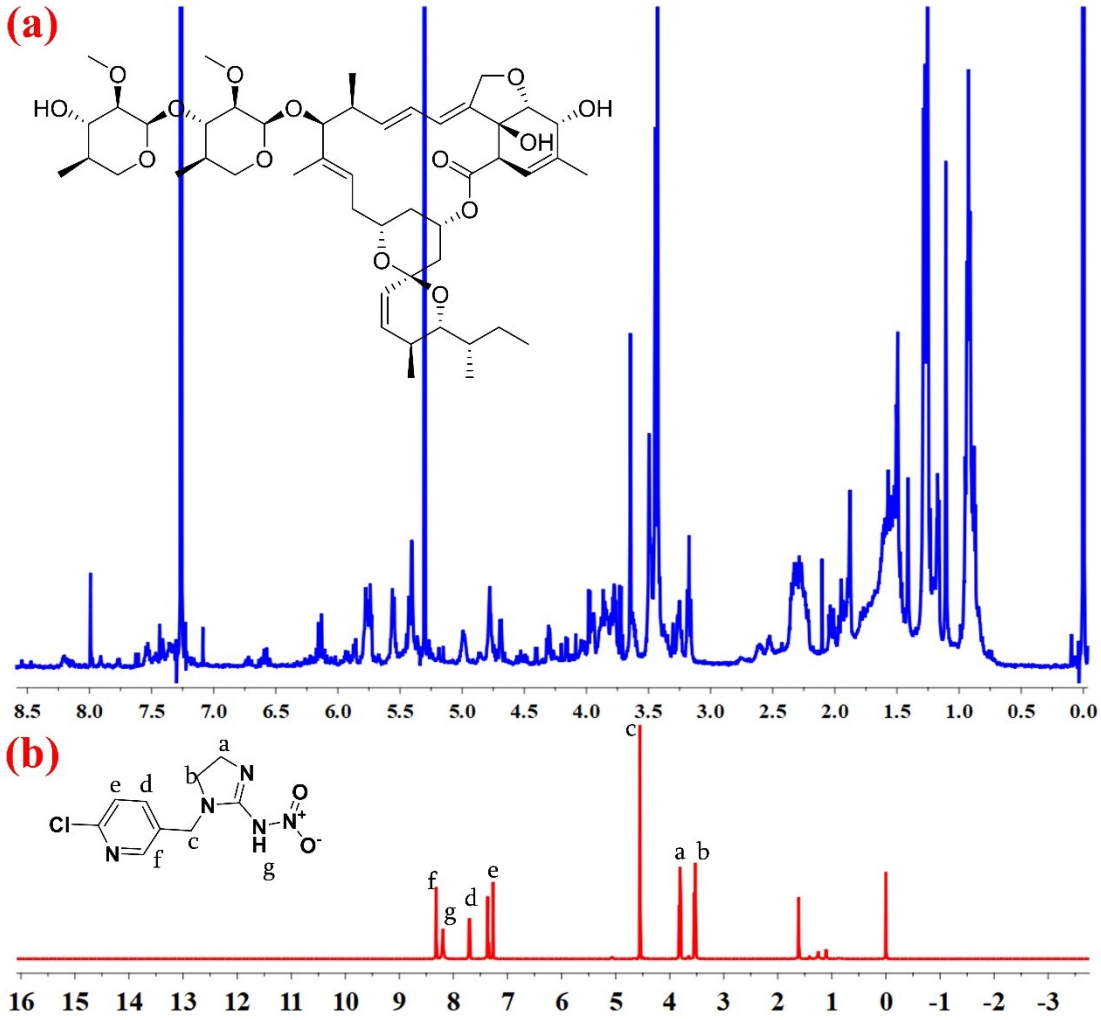

Fig. S1. ^{1}H NMR spectroscopy of AVM (a) and IMI (b)

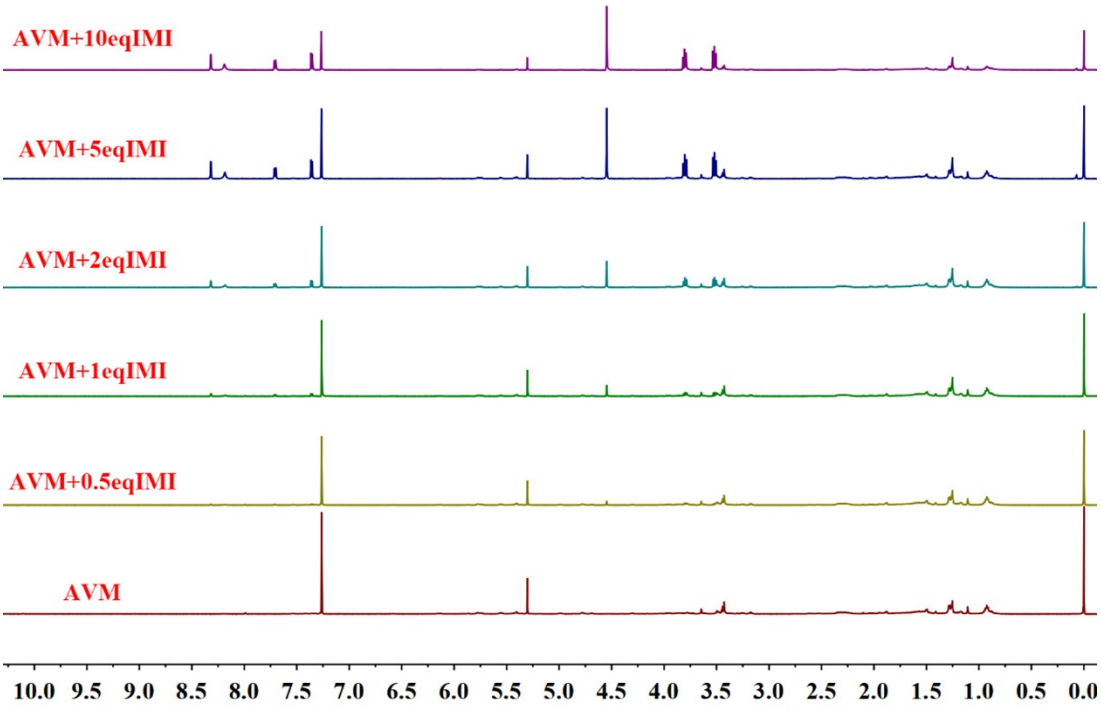

Fig. S2. The ^{1}H NMR full spectra of AVM in the absence and presence of increasing concentrations of IMI from 0 to 10 eq

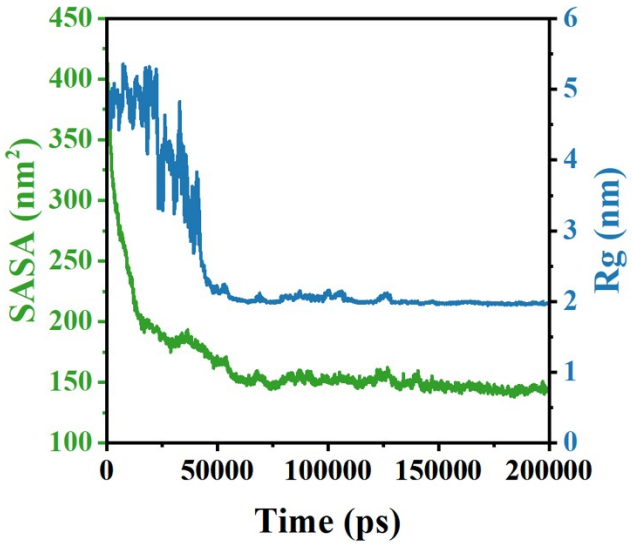

Fig. S3. Solvent-accessibility surface area (SASA) and radius of gyration (Rg) of AVM and IMI co-assembled molecular dynamics simulation

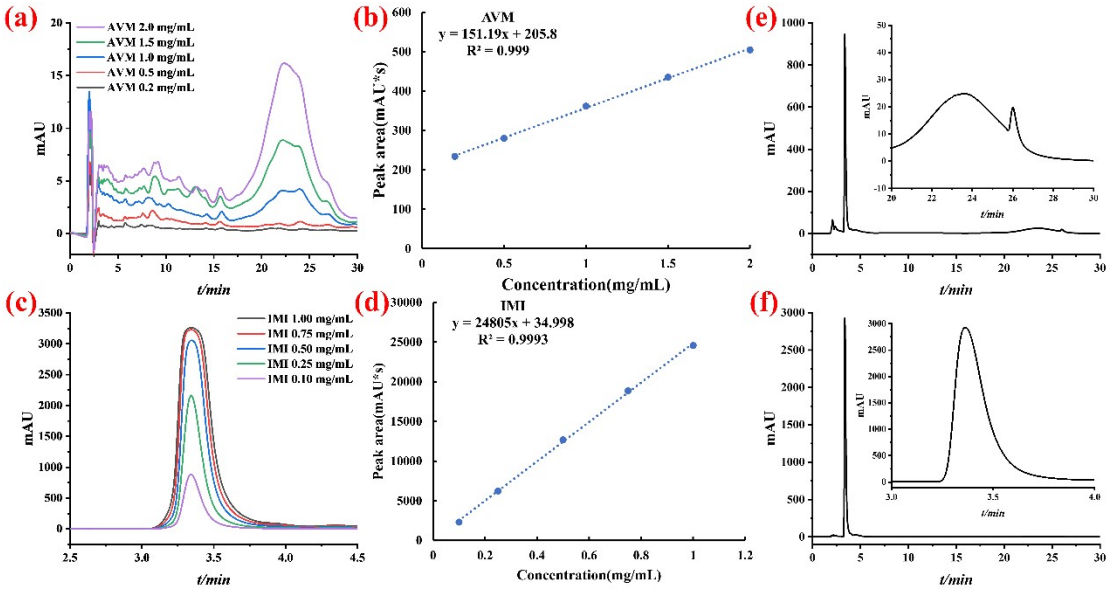

Fig. S4. HPLC chromatograms (a) and regression equation (b) of AVM (245 nm), HPLC chromatograms (c) and regression equation (d) of IMI (270 nm), and HPLC chromatograms for detection of AVM@IMI at 245 nm (e) and 270 nm (f)

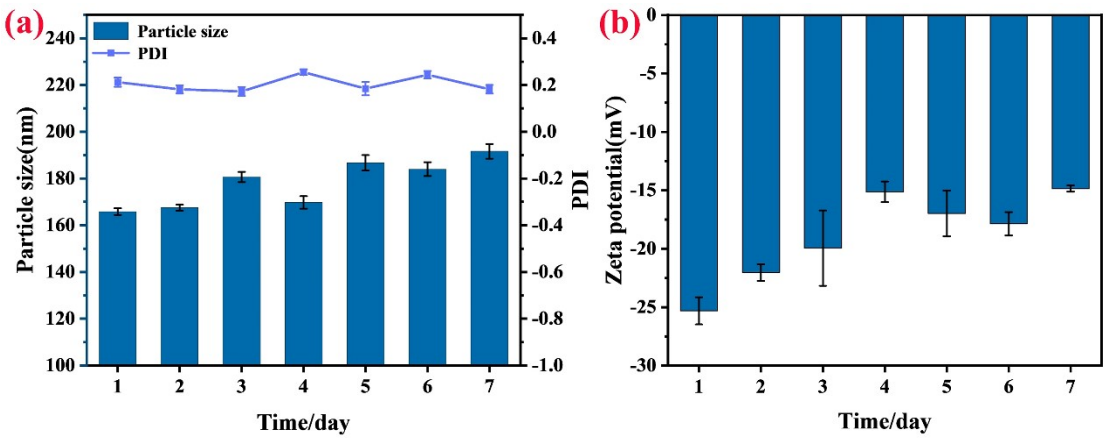

Fig. S5. The particle size and PDI (a) and Zeta potential (b) of AVM@IMI

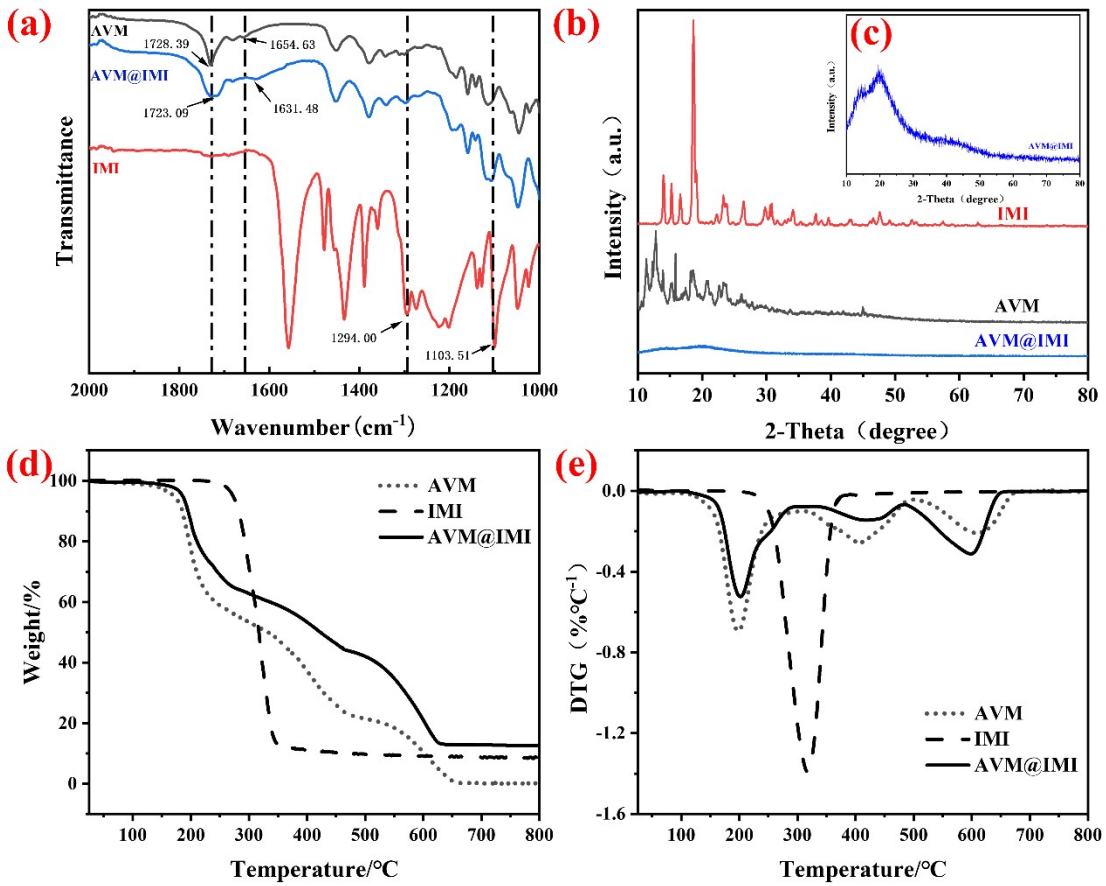

Fig. S6. The FT-IR spectra (a), XRD spectra (b and c), TG (d) and DTG (e) curves of AVM, IMI and AVM@IMI

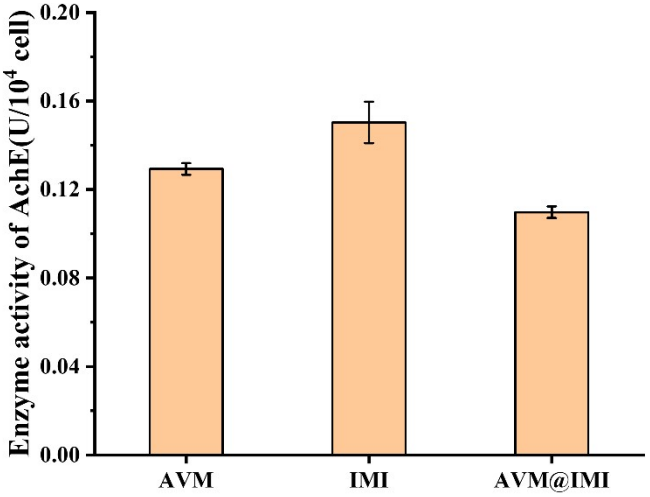

Fig. S7. Effects of AVM, IMI and AVM@IMI on AchE activity of *D. destructor.* (AchE: acetylcholinesterase)

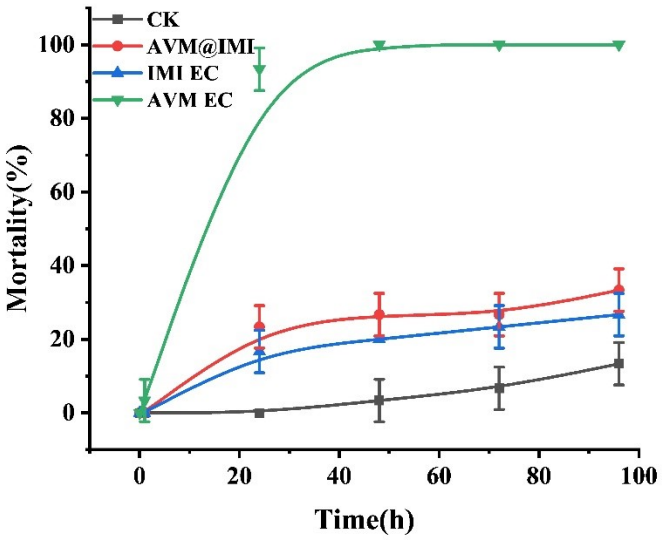

Fig. S8. Curves for the occurrence of mortality in zebrafish (*D. rerio*). *D. rerio* were exposed to AVM@IMI, IMI EC and AVM EC suspensions for 1, 24, 48, 72 and 96 h.

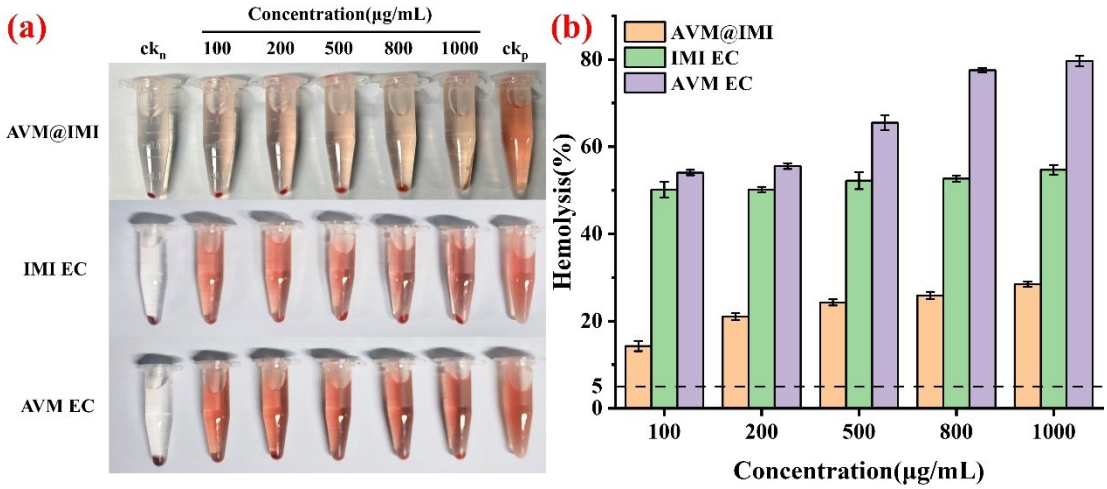

Fig. S9. Hemolysis effect pictures (a) and hemolysis rates (b) of AVM@IMI, AVM EC and IMI EC. The negative and positive controls were represented by ck_n and ck_p. (According to the Pharmaceutical industry standard of the People's Republic of China (YY/T 1651.1-2019), a determination result of hemolysis rate greater than 5% indicates that the test sample has hemolytic effect.)

Table S1. Abbreviation table

Abbreviation	Full name
AVM	Abamectin B1a
IMI	Imidacloprid
AVM@IMI	The self-assembled product of abamectin and imidacloprid
D. destructor	*Ditylenchus destructor*
DMSO	Dimethyl sulfoxide
HPLC	High performance liquid chromatography
SEM	Scanning electron microscope
FT-IR	Fourier transform infrared spectroscopy
XRD	X-ray diffractometer
AchE	Acetylcholinesterase
D. rerio	*Danio rerio*
H&E staining	Hematoxylin-eosin staining

Table S2. Information about the soil

Properties	Description	Method
pH	7.5~8.5	1
The content of organic matter	0.63%	2
The content of calcium carbonate	12%	3
The total salt content	0.074%	4

1 The pH value of the soil was tested in accordance with HJ 962-2018. Among them, the collection, preparation and preservation of soil samples referred to HJ/T 166. This method was called the point method. Simply put, when water was used as the leaching agent and the water-to-soil ratio was 2.5:1, the indicator electrode and the reference electrode were immersed in the soil suspension to form a primary cell. At a certain temperature, its electromotive force was related to the pH value of the suspension. By measuring the electromotive force of the primary cell, the pH value of the soil could be obtained.

2 The determination of organic matter content in soil was based on NY/T 4606-2025. The total carbon and organic matter content of soil samples were determined by the elemental analyzer method through high-temperature combustion oxidation.

3 The content of calcium carbonate in the soil was determined in accordance with the method in GB 9835-1988. The mass of calcium carbonate contained in the soil was obtained by converting the volume of carbon dioxide gas produced by the reaction of soil samples with hydrochloric acid.

4 The total salt of the soil was tested according to GB 15618-2018. There are two methods for determining the total salt content, namely gravimetric method and chemical analysis method. The gravimetric method involves drying soil samples in a drying oven and then determining the salt content in the soil based on the mass loss of the sample. Chemical analysis method involves determining the salt content in soil samples through steps such as water extraction, evaporation, drying and weighing.

Table S3. Acetylcholinesterase assay procedure

Reagent (μL)	Measuring tube	Contrastive tube
Sample	30	30
Reagent II	100	-
Accurately react for 5 min in 37 ℃ water bath		
Reagent IV	100	100
Reagent II	-	100
After mixing and centrifuging at 12000 rmp for 5 min at room temperature, 50 μL supernatant was taken into a new EP tube.		
Reagent I	850	850
Reagent III	100	100
After standing for 2 min, the absorbance of measuring tube and contrastive tube at 412 nm was recorded as A_m and A_c, respectively, and ΔA ($\Delta A = A_m - A_c$) was calculated.		

Table S4. The interaction between components in relevant studies

Components	Interaction force	Reference number
Glycyrrhizic acid + Spinosad	Hydrogen bonding, electrostatic interactions and van der Waals forces	1
Prochloraz + Fenhexamid	Electrostatic interactions, π–π stacking and hydrogen bonds	2
Tebuconazole + poly (salicylic acid)	Electrostatic interactions, π–π stacking and hydrogen bonds	3
Acifluorfen + poly (salicylic acid)	Hydrogen bonds, π–π stacking, and hydrophobic forces	4
Diphenylalanine + Fluroxypyr	Hydrogen bonding, electrostatic interactions, π–π stacking, hydrophobic interactions and van der Waals forces	5
Myclobutanil + Tannic acid	Hydrogen bonds, π–π stacking, and hydrophobic forces	6
Azadirachtin + tannic acid or phenylalanine	π–π stacking, and hydrophobic forces	7

In related research, the interaction forces among the components are mainly hydrogen bonding, electrostatic interactions, π-π stacking, hydrophobic interactions and van der Waals forces. However, the π-alkyl interactions in this study have rarely been studied.

1. K. Wei, Z. Li, Z. Zheng, Y. Gao, Q. Huang, M. Li and J. Hu, Natural Glycyrrhizic Acid-Tailored Nanoparticles toward the Enhancement of Pesticide Bioavailability, *Advanced Functional Materials*, 2024, **34**.
2. Z. Zhou, G. Tang, Y. Liu, Y. Huang, X. Zhang, G. Yan, G. Hu, W. Yan, J. Li and Y. Cao, Carrier-free self-assembled nanoparticles based on prochloraz and fenhexamid for reducing toxicity to aquatic organism, *Science of the Total*

Environment, 2024, **943**.

3. Y. Huang, H. Wang, G. Tang, Z. Zhou, X. Zhang, Y. Liu, G. Yan, J. Wang, G. Hu, J. Xiao, W. Yan and Y. Cao, Fabrication of pH-responsive nanoparticles for co-delivery of fungicide and salicylic acid with synergistic antifungal activity, *Journal of Cleaner Production*, 2024, **451**.
4. H. Wang, G. Tang, Z. Zhou, X. Chen, Y. Liu, G. Yan, X. Zhang, X. Li, Y. Huang, J. Wang and Y. Cao, Stable Fluorescent Nanoparticles Based on Co-assembly of Acifluorfen and Poly(salicylic acid) for Enhancing Herbicidal Activity and Reducing Environmental Risks, *Acs Applied Materials & Interfaces*, 2023, **15**, 4303-4314.
5. Z. Zheng, Z. Yang, Z. Meng, S. Liu, T. Wu, C. He, C. Zhang, C. Ma, Y. Gao and F. Du, Sustainable nanocarriers fabricated via a dipeptide-based co-assembly approach for enhancing the delivery and translocation of herbicides, *Environmental Science-Nano*, 2025, **12**, 686-700.
6. X. Li, Z. Zhou, Y. Huang, G. Tang, Y. Liu, X. Chen, G. Yan, H. Wang, X. Zhang, J. Wang and Y. Cao, A high adhesion co-assembly based on myclobutanil and tannic acid for sustainable plant disease management, *Pest Manage. Sci.*, 2023, **79**, 3796-3807.
7. X. Zhang, J. Xiao, Y. Huang, Y. Liu, G. Hu, W. Yan, G. Yan, Q. Guo, J. Shi, R. Han, J. Li, G. Tang and Y. Cao, Sustainable pest management using plant secondary metabolites regulated azadirachtin nano-assemblies, *Nature Communications*, 2025, **16**.

Table S5. The results of elemental analysis of AVM@IMI

	N (w/%)	C (w/%)	H (w/%)	AVM (w/%)	IMI (w/%)
AVM	0	62.19	7.7295	100	0
IMI	27.53	42.345	3.8795	0	100
AVM@IMI	5.615	58.37	6.740	71	29